J. Plasma Physics (2006), *vol.* 72, *part* 6, *pp.* 1223–1227. © 2006 Cambridge University Press
doi:10.1017/S0022377806005988 Printed in the United Kingdom

Nonlinear three-dimensional simulations of resistive wall modes

M. SATO and N. NAKAJIMA

National Institute for Fusion Science, Toki, 509-5292, Japan

(Received 15 August 2005 and accepted 9 February 2006)

Abstract. Nonlinear behavior of the resistive wall modes (RWMs) has been studied using nonlinear three-dimensional simulation code based on the reduced magnetohydrodynamic equations in a cylindrical tokamak. The vacuum is replaced by a highly resistive plasma using the pseudo-vacuum model. For the case that the RWM with $(m, n) = (3, 1)$ mode and the internal $(m, n) = (5, 2)$ mode are unstable, the RWM with $(m, n) = (3, 1)$ mode enhances the growth rate of the internal $(m, n) = (5, 2)$ mode in the nonlinear phase. The magnetic field line stochastization is obtained around the plasma edge due to the overlapping of the magnetic islands of the $(m, n) = (3, 1)$ mode and the $(m, n) = (5, 2)$ mode.

1. Introduction

For obtaining high beta plasma in tokamaks, stabilization of external kink modes is required. The external kink modes can be stabilized perfectly by locating a perfect conducting wall sufficiently close to the plasma surface. However, when the wall has a finite conductivity, the mode cannot be stabilized perfectly and the slowly growing resistive wall modes (RWMs) appear [1]. Experimentally, it is found that plasmas exceeding no-wall β limit are obtained for time periods much longer than the diffusion time of the resistive wall [2,3]. In these experiments, there is a rapid toroidal rotation due to unbalanced neutral beam injection. Theoretically, it is shown that the combination of plasma rotation and some dissipation model can stabilize RWMs [4–7]. When the RWMs are destabilized, the RWM results in major collapse. For the nonlinear phenomena, the effect of mode coupling is important, such as the toroidal coupling and the nonlinear mode coupling with other unstable modes. In this paper, we study the effect of nonlinear mode coupling of the RWM and other unstable modes by means of nonlinear three-dimensional simulation for a low beta cylindrical tokamak.

2. Numerical model

For studying the RWMs, the following reduced magnetohydrodynamic (MHD) equations [8,9] are solved numerically in the cylindrical coordinates (r, θ, ζ):

$$\frac{\partial \psi}{\partial t} = -\mathbf{B} \cdot \nabla \phi + \eta J - E, \tag{2.1}$$

$$\frac{\partial U}{\partial t} = \mathbf{v} \cdot \nabla U + \frac{1}{2}[\rho, v^2] - \mathbf{B} \cdot \nabla J - \mathbf{e}_z \cdot \nabla \times \nabla \cdot \boldsymbol{\pi} + S_{\mathrm{m}}, \tag{2.2}$$

https://doi.org/10.1017/S0022377806005988 Published online by Cambridge University Press

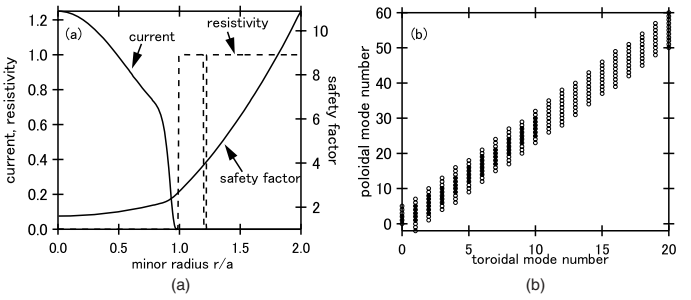


Figure 1. (a) Radial profiles of safety factor q, plasma current density J, and resistivity η at equilibrium state. (b) The (m, n) modes chosen for ψ, ϕ, J and U marked by '●' and those for η marked by '●' and '○'.

$$\frac{\partial T}{\partial t} = \mathbf{v}_\perp \cdot \nabla T, \quad \frac{\partial \rho}{\partial t} = \mathbf{v}_\perp \cdot \nabla \rho, \quad \mu_0 J = \nabla_\perp^2 \psi, \quad U = \nabla \cdot (\rho \nabla_\perp \phi),$$

where

$$[f, g] = \frac{1}{r}\frac{\partial f}{\partial r}\frac{\partial g}{\partial \theta} - \frac{1}{r}\frac{\partial f}{\partial \theta}\frac{\partial g}{\partial r},$$

ψ is the poloidal magnetic flux defined by $\mathbf{B} = -\nabla\psi \times \mathbf{e}_z + B_0 \mathbf{e}_z$, ϕ is the stream function defined by $\mathbf{v}_\perp = \nabla\phi \times \mathbf{e}_z$, T is temperature, ρ is density and Spitzer resitivity is assumed, i.e., $\eta \propto T^{-3/2}$. In (2.2), the shear viscosity is assumed and $\boldsymbol{\pi}$ is defined by $\boldsymbol{\pi} = \nu\rho(\nabla \mathbf{v} + \nabla \mathbf{v}^{\mathrm{t}})$. We assumed that there is not equilibrium flow so that the momentum source term S_{m} is set to be $S_{\mathrm{m}} = 0$. For treating external MHD modes, a highly resistive plasma is introduced in the vacuum region to use the pseudo-vacuum model [10,11]. The ratio of the resistivity in the highly resistive plasma η_v to one at the center η_0 is chosen as $\eta_v/\eta_0 = 10^7$ for nonlinear simulation. The magnetic Reynolds number $S = \tau_a/\tau_r$ is set to be $S = 10^7$, where $\tau_a = R\sqrt{\mu_0\rho_0}/B_0$, $\tau_r = \mu_0 a^2/\eta_0$, ρ_0 is density at $r = 0$, R is major radius of the plasma and a is minor radius of the core plasma. The highly resistive plasma is surrounded by a resistive wall located at $r = r_{\mathrm{w}}$. Another highly resistive plasma is located outside the resistive wall. For the resistive wall and the outer highly resistive plasma outside the resistive wall, the resistivity does not change and the velocity is zero. Therefore, the diffusion equation of the perturbed poloidal magnetic flux $\tilde{\psi}$, $\partial\tilde{\psi}/\partial t = \eta J$, is solved in the resistive wall and the outer highly resistive plasma. It is assumed that the outer highly resistive plasma is covered by a perfect conducting wall at $r_{\mathrm{d}} = 2a$ for simplicity.

In this paper, we use the following current profile to study the RWMs of the $(m, n) = (3, 1)$ mode:

$$J_{\mathrm{eq}}(r) = (J_0 - J_v)(0.48(1 - (r/a)^2)^2 + 0.52)(1 - (r/a)^{30})^{10} + J_v \qquad (2.3)$$

for $0 \leqslant r \leqslant a$, and $J_{\mathrm{eq}}(r) = J_v \ll J_0$ for $a < r$. The profiles of safety factor q, current J_{eq} and resistivity η_{eq} at equilibrium state are shown in Fig. 1(a). The resistivity profile is assumed to be proportional to $1/J_{\mathrm{eq}}(r)$ for $r < r_{\mathrm{w}}$. The density profile for

https://doi.org/10.1017/S0022377806005988 Published online by Cambridge University Press

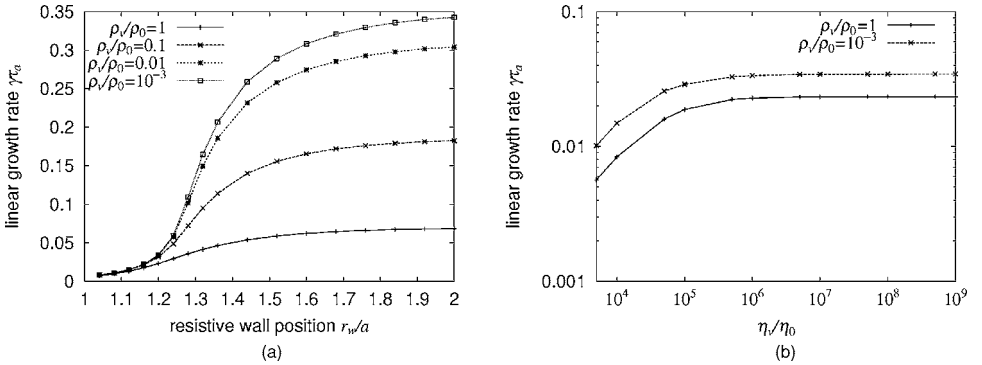


Figure 2. (a) Dependence of linear growth rate on resistive wall position $r_{\rm w}$ for $\eta_v/\eta_0 = 10^7$. (b) Dependence of linear growth rate on the resistivity of the external highly resistive plasma for $r_{\rm w} = 1.2a$.

$r < r_{\rm L} = 0.95$ is determined from the equilibrium equation

$$\rho(\mathbf{v}\cdot\nabla)\mathbf{v} = -\nabla P + \mathbf{J}\times\mathbf{B}, \tag{2.4}$$

where $P \propto \rho T$. The density profile is chosen as monotonically decreasing function for $r_{\rm L} < r < a$ and $\rho_{\rm eq}(r) = \rho_v$ for $r > a$, where ρ_v is density of the highly resistive plasma. Thus, the equilibrium equation (2.4) is not satisfied near the plasma surface. However, since the initial profile depends on only minor radius r, it is maintained unless a perturbation is added.

For solving (2.1) and (2.2) in our numerical code, the radial derivatives are replaced with standard difference approximations and the derivatives with respect to the angle is treated with Fourier–expansions. The time advancement is made with a predictor–corrector method. The diffusion term in the (2.1) is treated implicitly. For solving equations of T and ρ, we use the RCIP (Rational Constrained Interpolation Profile or Rational Cubic Interpolated Pseudo-particle) method [12]. In the CIP (Constrained Interpolation Profile) of Cubic Interpolated Pseudo-particle) method [13], not only the variable (T) but also the first-order derivatives of the variables ($\partial T/\partial r$, etc.) are solved. The standard CIP method uses a cubic polynomial function and the RCIP method uses a rational function to construct the interpolating function. The RCIP method is attractive in suppressing the numerical oscillation near a discontinuity. For nonlinear multi-simulation in this paper, the radial mesh number is 500 and 55 fourier modes are used for ψ, J, ϕ and U, and 210 fourier modes for η as shown in Fig. 1(b). For the RCIP method, the poloidal mesh number and the toroidal mesh number are 160 and 60, respectively.

3. Numerical results

Figure 2(a) shows the dependence of the linear growth rate on the resistive wall position $r_{\rm w}$ for various densities of the highly resistive plasma, where $\eta_v/\eta_0 = 10^7$ is assumed. The linear growth rate of the RWMs ($r_{\rm w} \lesssim 1.3a$) does not depend on the density of the highly resistive plasma, since the inertia term can be neglected for the slowly growing RWMs. Figure 2(b) shows the dependence of the linear growth rate on the resistivity of the highly resistive plasma, where the resistive wall is located at $r_{\rm w} = 1.2a$ and the density profile is constant, i.e. $\rho_v = \rho_0$. For $\eta_v/\eta_0 > 10^5$, the

https://doi.org/10.1017/S0022377806005988 Published online by Cambridge University Press

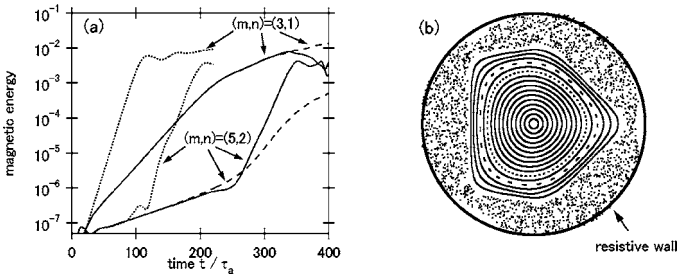


Figure 3. (a) Time evolution of magnetic energies of $(m,n)=(3,1)$ and (5,2) components. The solid, the dotted and broken lines correspond to results for the multi-helicity case with a resistive wall, multi-helicity case without a resistive wall, and the single helicity case with the resistive wall, respectively. (b) Field line plots at $t=330\tau_a$ for multi heliciy case for $r_{\rm w}=1.2a$.

linear growth rate does not depend on η_v. Therefore, the value of $\eta_v/\eta_0=10^7$ is sufficiently large for analyzing the external mode.

For the equilibrium profile as shown in Fig. 1(a), the rational surface with $q=\frac{5}{2}$ is located at $r=0.96a$ and the internal $(m,n)=(5,2)$ mode is also unstable. Figure 3(a) shows time evolution of magnetic energies of the $(m,n)=(3,1)$ mode and the $(m,n)=(5,2)$ mode. The solid, the dotted and broken curves correspond to results for the multi-helicity case with the resistive wall located at $r_{\rm w}=1.2a$, multi-helicity case without a resistive wall, and the single helicity case with the resistive wall located at $r_{\rm w}=1.2a$, respectively. The $(m,n)=(5,2)$ mode is strongly destabilized in the nonlinear phase for all cases. For the single helicity case, the same phenomenon was obtained for $(m,n)=(2,1)$ mode in [11]. However, the enhanced growth rate of the $(m,n)=(5,2)$ mode for the multi-heiclity case is larger than that for the single helicity case. When the magnetic energy of the $(m,n)=(5,2)$ mode is comparable to that of the $(m,n)=(3,1)$ mode, the edge plasma region becomes the magnetic field stochastic region as shown in Fig. 3(b). We also carried out nonlinear simulation for $r_{\rm w}=1.2a$ using 105 Fourier modes for ψ, J, ϕ and U, and 405 Fourier modes for η. We obtained the same result about destabilizing the $(m,n)=(5,2)$ mode.

4. Conclusions

Nonlinear simulation of the RWMs has been carried out using the reduced MHD equations in a low beta cylindrical tokamak. The core plasma with low resistivity is surrounded by the highly resistive plasma. In this paper, we use the equilibrium profile where the RWM with $(m,n)=(3,1)$ and the internal $(m,n)=(5,2)$ mode are linearly unstable. The internal $(m,n)=(5,2)$ mode is strongly destabilized in the nonlinear phase. The enhanced growth rate for the multi-helicity case is larger than that for the single helicity case. The overlapping of the islands of the $(m,n)=(3,1)$ mode and $(m,n)=(5,2)$ mode results in magnetic field line stochastic behavior. It may cause to destabilize other internal modes such as $(m,n)=(2,1)$ mode and a disruption due to changing of the current profile near the edge of the plasma. The study of the long time simulation is our future work.

https://doi.org/10.1017/S0022377806005988 Published online by Cambridge University Press

Acknowledgement

This work is supported by Research Fellowships of the Japan Society for the Promotion of Science for Young Scientists.

References

[1] Pfirsch, D. and Tasso, H. 1971 *Nucl. Fusion* **11**, 259–260.
[2] Taylor, T. S. et al. 1995 *Phys. Plasmas* **2**, 2390–2396.
[3] Strait, E. J. et al. 1995 *Phys. Rev. Lett.* **74**, 2483–2486.
[4] Bondeson, A. and Ward, D. 1994 *Phys. Rev. Lett.* **72**, 2709–2712.
[5] Betti, R. and Freidberg, J. P. 1995 *Phys. Rev. Lett.* **74**, 2949–2952.
[6] Chu, M. S. et al. 1995 *Phys. Plasmas* **2**, 2236–2241.
[7] Fitzpatrick, R. and Aydemir, A. 1996 *Nucl. Fusion* **36**, 11–38.
[8] Kadomtsev, B. B. and Pogutse, O. P. 1974 *Sov. Phys.–JETP* **38**, 283–290.
[9] Strauss, H. R. 1976 *Phys. Fluids* **19**, 134–140.
[10] Dnestrovskii, Yu. N. et al. 1985 *Sov. J. Plasma Phys.* **11**, 616–621.
[11] Kurita, G. et al. 1986 *Nucl. Fusion* **26**, 449–460.
[12] Xiao, F., Yabe, T. and Ito, T. 1996 *Comput. Phys. Commun.* **93**, 1–12.
[13] Yabe, T. and Aoki, T. 1991 *Comput. Phys. Commun.* **66**, 219–232.

https://doi.org/10.1017/S0022377806005988 Published online by Cambridge University Press